Experimental verification of Herring's theory of anharmonic phonon relaxation: TeO_2

E. P. N. Damen, A. F. M. Arts, and H. W. de Wijn
Faculty of Physics and Astronomy, and Debye Research Institute, Utrecht University, P.O. Box 80.000, 3508 TA Utrecht, The Netherlands
(Received 6 July 1998)

The attenuation of a narrow Fresnel-diffracted monochromatic beam of longitudinal phonons propagating along the [001] axis is measured as a function of the frequency and the temperature in a single crystal of paratellurite (TeO_2). The attenuation varies according to $\omega^a T^b$ with $a=1.84\pm0.20$ and $b=2.81\pm0.20$ below about 53 K, and according to $\omega^a T$ with $a=1.87\pm0.20$ above this temperature. These results confirm Herring's theory for anharmonic phonon decay in anisotropic crystals, with $\mathsf{L}+\mathsf{ST}\rightarrow\mathsf{FT}$ the relevant three-phonon process. [S0163-1829(99)09501-6]

I. INTRODUCTION

In a seminal paper on the role of phonons in thermal conduction, written to remove the divergence of the conductivity predicted for perfect crystals, Herring[1] has pointed out that anharmonic phonon decay is profoundly dependent on the elastic anisotropy of the medium. In particular, he showed that at low temperatures the decay rate τ^{-1} of longitudinal phonons against three-phonon processes depends on the angular frequency ω and temperature T as $\tau^{-1} \propto \omega^a T^b$, in which the exponent a is determined by the crystal class, the direction of the phonon wave vector, and the presence of dispersion, while $a+b=5$. The prevailing a equals 2, 3, or 4. Despite an abundance of experimental material on phonon scattering in solids,[2–4] direct experimental verification of Herring's theory has remained elusive, primarily because of the scarcity of phonon sources delivering a phonon beam of well-defined frequency and wave vector. Thermal conduction, by its nature, depends on temperature-weighted summation over all frequencies of a variety of phonon processes. Facing this problem of considerable complexity, theoretical treatments[5–7] usually assume the $a+b=5$ rule to be valid, and in keeping with this rule adopt frequency and temperature dependences for the various phonon relaxation rates. For relaxation of longitudinal phonons by normal processes the dependence $\tau^{-1}\propto\omega^2 T^3$ is commonly taken. These choices are generally found to lead to a consistent description of the experiment.[8–10]

A more stringent verification of Herring's theory requires a determination of the exponents a and b by direct measurement of the phonon decay versus the temperature at well-defined frequencies, preferably in the ballistic regime and undisturbed by boundary effects. In the present paper this is achieved by making use of a recently developed technique for the generation of monochromatic Fresnel-diffracted phonon beams in the gigahertz range.[11] The method relies on cw laser-induced thermomodulation of a metallic transducer evaporated onto the crystal, and permits measurement as a function of T at various ω. In addition to monochromaticity and tunability, the technique features substantial narrowness of the phonon beam with minimum divergence. In combination with detection by Brillouin scattering, which is wave-vector selective, diffusive processes and thermal background are therefore largely eliminated. The validity of Herring's results thus is established for a system of intermediate symmetry, viz., a single crystal of paratellurite (TeO_2) at sufficiently low temperatures ($\lesssim 100$ K). TeO_2 was chosen for its strongly anisotropic transverse phonon branches and its high Brillouin yield.

II. EXPERIMENTS

The specimen was a single crystal of synthetic TeO_2, $10.5\times9.5\times10$ mm^3 in size (obtained from Isomet Corporation). For the sake of phonon generation, a gold transducer consisting of steps of four different thicknesses (220–660 nm) was deposited onto an outer surface oriented according to (001). A highly directional monochromatic phonon beam of longitudinal polarization, only 40 μm in diameter, with a divergence of about 2°, and propagating along [001], was generated by modulated heating of the transducer surface.[11] This thermomodulation is brought about by two interfering cw single-frequency ring dye lasers, operating with Rhodamine 6G dye at 580-nm wavelength, and, so as to avoid phase differences over the excitation area, aligned such that their beams are collinear. The thermomodulation causes a strain at the laser difference frequency, which ultimately is injected into the crystal. Self-evidently, the generated phonons are of longitudinal polarization. The transducer thickness was chosen such as to benefit from acoustic resonances. A helium-gas-flow cryostat was used. A thermometer near the crystal monitored the actual temperature.

The acoustic attenuation was measured as a function of the temperature with reliance on Brillouin scattering, i.e., one-phonon inelastic scattering, for various phonon frequencies (3.0, 3.2, 3.7, 4.1, 4.2, 4.9, and 5.0 GHz, with an error margin of 0.1 GHz) and various distances from the transducer. Brillouin spectroscopy was adopted because it permits *in situ* measurement of the phonon density in a restricted volume, and because it is selective for both the frequency and the wave vector, thereby minimizing the background by residual diffusion and thermal phonons. In the present arrangement, the Brillouin condition selects wave vectors within a cone of about 1°. The Brillouin spectrometer is of conventional design. The primary light beam, suitably polarized and focused to a pencil as narrow as 10 μm in diameter,

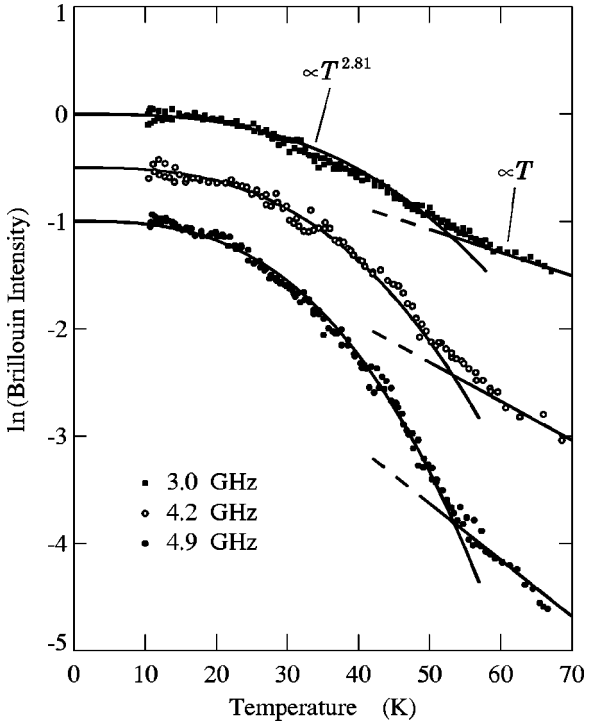

FIG. 1. Logarithm of the Brillouin intensity, i.e., $z/v\tau$, arising from acoustic phonons in TeO_2 versus the temperature. The intensity was collected in a 10-μm diameter volume at a distance of 2.0 mm from the transducer for phonon frequencies of 3.0, 4.2, and 4.9 GHz. The data at 4.2 and 4.9 GHz are shifted downward for clarity. The curves and straight lines represent the low-temperature dependence Eq. (1) and the high-temperature dependence Eq. (2), with the parameters resulting from the overall fit inserted.

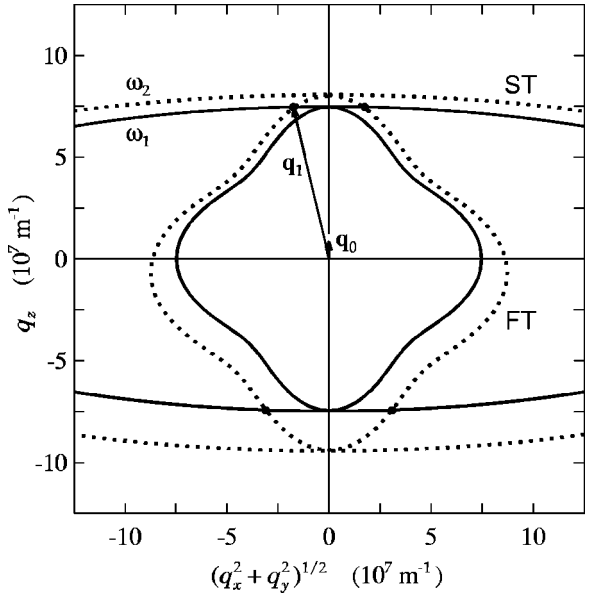

FIG. 2. Constant-energy contours of FT and ST phonons in TeO_2. The figure shows the central part of a (110) plane in **q** space. The full contours refer to the ST and FT phonon branches of frequency $\omega_1/2\pi = 25.0$ GHz, the dotted contours similarly to 29.2-GHz phonons. The 29.2 GHz branches are shifted over minus the wave vector $\mathbf{q}_0$ of 4.2-GHz L phonons propagating along [001]. The locus $\mathbf{q}_1$ of their intersection with the 25.0-GHz branches (black dots) satisfies both momentum and energy conservation in the process L+ST→FT.

is provided by an argon-ion laser beam operating at 514.5 nm wavelength. The scattered anti-Stokes light emerging from a small volume selected by the primary beam and the detection optics is frequency-selectively analyzed by the use of an actively stabilized quintuple-pass Fabry Perot interferometer (Burleigh RC-110), passed through a monochromator to eliminate laser plasma lines, detected by a photomultiplier, and finally stored repetitively by standard photon counting techniques.

The intensity of the scattered Brillouin light, which is a direct measure of the acoustic power of the phonon beam, was measured at a fixed position below the transducer. For each frequency and distance, the temperature was increased from 10 K upward in small steps. Figure 1 shows a few examples of the results. After completion of a temperature scan the sample was cooled down to the starting temperature, to verify that the optics and other settings had not changed. A total of 17 fixed-frequency variable-temperature scans were performed, some of them extending beyond 100 K. Most data were taken at a depth of 2.0 mm below the transducer.

At one frequency (4.1 GHz), data were collected at distances of 0.5, 1.0, 2.0, 3.0, and 4.0 mm. When extrapolated to zero distance, these data reflect the variation of the phonon generation efficiency with the temperature. It is important to consider this variaton, because it adds to the phonon-associated decrease of the Brillouin intensity. A detailed analysis, however, shows that at 50 K the generation efficiency has dropped by only (5±5) %, the effects of which are well within the uncertainties from other sources.

III. PHONON DECAY

Energy as well as wave-vector conserving scattering due to the lattice anharmonicity, in which a phonon combines with a thermal phonon to form a phonon of larger energy, presumably is the dominant mechanism of phonon decay in pure single crystals.[2–4] At very low temperatures, therefore, the generated longitudinal phonons travel virtually ballistically, but their mean free path shortens when the temperature is raised.

In elastically isotropic media, the anharmonic processes a longitudinal phonon suffers on its travel are L+T→L and L+L→L, where L and T denote longitudinal and transverse phonons. The decay rate associated with the process L+T→L depends on the frequency and the temperature according to $\tau^{-1} \propto \omega^4 T$ for $\hbar\omega \ll k_B T$, in which τ is the single-mode relaxation time.[4] For the process L+L→L similarly $\tau^{-1} \propto \omega T^4$, but here the three wave vectors must be collinear, and some sort of dressing of the states is necessary to overcome the slight energy mismatch due to dispersion.[12,13] Obviously, none of these processes is in conformity with the experiment.

In real media, which are elastically anisotropic, the scattering of low-energy longitudinal phonons is profoundly different by dominance of yet another process, as was first pointed out by Herring.[1] The arguments are of topological and group-theoretical nature. For the present case of longitudinal acoustic phonons propagating along [001] in TeO_2 this is illustrated in Fig. 2. The figure, which results from solving

the Christoffel equations[2] with known elastic constants,[14–16] and covers the central part of the (110) plane in the Brillouin zone, shows constant-energy contours for the fast-transverse (FT) and slow-transverse (ST) phonon branches. Let us consider the process $L+ST\rightarrow FT$, which is forbidden in isotropic crystals, and let us denote the wave vectors of the three phonons by $\mathbf{q}_0$, $\mathbf{q}_1$, and $\mathbf{q}_2$, and similarly their angular frequencies by ω_0, ω_1, and ω_2. Here, $\mathbf{q}_0$ denotes the wave vector of the relaxing longitudinal phonon, propagating along [001]. The locus of the $\mathbf{q}_1$'s simultaneously satisfying conservation of momentum, $\mathbf{q}_0+\mathbf{q}_1=\mathbf{q}_2$, and energy, $\omega_0+\omega_1=\omega_2$, can then be constructed by shifting the ω_2 contour in $\mathbf{q}$ space over a distance $-\mathbf{q}_0$ (dotted lines in Fig. 2), and determining the intersection of this contour with the unshifted ω_1 contour (black dots in Fig. 2). The locus forms curved lines in three-dimensional $\mathbf{q}$ space, with $\mathbf{q}_1$ in the near forward direction or near backward direction.

Using group-theoretical considerations, Herring has worked out the asymptotic, i.e., the small wave vector, ω and T dependences of the associated phonon decay rate τ^{-1}. Quite generally,

$$\tau^{-1}=A\omega^a T^b, \tag{1}$$

with $a+b=5$ on the proviso that $\mathbf{q}_0$ is in the acoustic regime and that T is well below the Debye temperature. In the limit of high temperatures, however, where all phonon modes are appreciably excited,

$$\tau^{-1}=B\omega^a T. \tag{2}$$

Herring has furthermore argued that, apart from collinear decay, the process with the lowest power of ω is dominant on account of the density of states. The major contribution to the attenuation of longitudinal phonons thus arises from the process $L+ST\rightarrow FT$, yielding $\tau^{-1}\propto\omega^a T^b$ at low, and $\tau^{-1}\propto\omega^a T$ at high temperatures. This, in fact, is what we wish to show experimentally.

IV. DATA ANALYSIS AND DISCUSSION

Before analyzing the data, we discuss what values of a and b are expected from Herring's theory on the basis of the crystal class. The crystal structure of TeO_2 has been examined in detail by Leciejewicz,[17] who used neutron diffraction to map out the atomic positions of the four formula units contained in the tetragonal unit cell, and to find that the space group is D_4^4, or $P4_12_1$. TeO_2 thus belongs to the crystal class D_4. According to Table II of Herring's paper this implies $a=4$, but $a=2$ in case phonon dispersion is negligible. As the relaxing phonons have their wave vector near the Brillouin-zone center, terms with $a=2$ thus dominate the relaxation.

A second circumstance favoring a quadratic ω dependence is that TeO_2 only minutely deviates from the more symmetric rutile structure (space group D_{4h}^{14}, or $P4/mmm$), which belongs to the crystal class D_{4h}. In fact, the unit cell of TeO_2 can be thought of as to consist of two c-axis stacked rutile unit cells with the atoms rearranged over distances of up to 0.03 lattice spacings. In the case of crystal class D_{4h} we have $a=2$ for any phonon frequency, because the transverse phonon branches have lines of degeneracy of Herring's type (iv) associated with points P all the way to the Brillouin-zone boundary.[18] Summarizing, for the present case of longitudinal acoustic phonons propagating along [001] in TeO_2 we expect $a=2$ and $b=3$.

In the detailed analysis of the data such as those in Fig. 1, necessary to extract the experimental exponents a and b in Eq. (1), the signal intensity is assumed to depend exponentially on the inverse relaxation time according to

$$I=I_0 e^{-z/v\tau}, \tag{3}$$

where z is the distance the acoustic wave has covered from the transducer, v is the sound velocity, and the zero-temperature intensities I_0 refer to the respective temperature scans. In other terms, $\ln_e(I/I_0)=-1$ corresponds to a mean free path equal to z, i.e., 2.0 mm in Fig. 1. For longitudinal phonons propagating along [001], we have $v=4.202\pm0.010$ km/s.[14]

After substituting Eq. (1) into Eq. (3), we have carried out a recursive multiparameter least-squares fit to all 17 temperature scans with a, b, A, and the I_0's as adjustable parameters. A good fit was obtained, provided the data are limited to temperatures below, say, 53 K (cf. Fig. 1). The output values for the coefficients are

$$a=1.84\pm0.20, \quad b=2.81\pm0.20.$$

We furthermore find $A=(4.0\pm0.5)\times10^{-18}$ $s^{a-1}\,K^{-b}$. In this analysis, the I_0's pertaining to a particular z, but various ω, could be interrelated in the limit of small damping, i.e., in the zero-temperature limit (cf. Fig. 1). Relating the I_0 for various z has not been attempted because this would involve substantial corrections for the effects of phonon focusing and the spreading out of the phonon beam by diffraction beyond the measuring volume.[11]

The experimental a and b are indeed in conformity with Herring's predictions, while their sum is close to five. To show the quality of the fit versus frequency and temperature, the quantity $z/v\tau$ is plotted in Fig. 1, as calculated from Eq. (1) with the fitted parameters inserted. To further demonstrate that Eq. (1) tracks the data points over the ranges of ω and T considered, we compare the ''measured'' τ^{-1} with the theoretical frequency and temperature dependence $A\omega^a T^b$, again with the fitted parameters inserted, for all 17 fixed-frequency temperature scans. Here, τ^{-1} is derived from the experimental I/I_0 and z through Eq. (3). The result is presented in Fig. 3, which is set up in such a way that collapse of the data on a single straight line signifies agreement.

We next consider the high-temperature regime. According to Herring,[1] Eq. (1) is valid only well below the Debye temperature, the attenuation becoming linear with the temperature when most phonon modes are thermally excited [cf. Eq. (2)]. No new mechanism is involved, but rather the temperature dependence changes over from cubic to linear, so the high-temperature attenuation should extrapolate to zero at zero temperature. This is indeed what is observed above about 53 K, as is shown in Fig. 1 for a selection of the data. A fit of Eq. (2), adjusting a, B, and the I_0 to all data from 53 to 100 K, yielded $a=1.87\pm0.20$,[19] to be compared with Herring's $a=2$. We furthermore find $B=(2.6\pm0.5)\times10^{-15}$ $s^{a-1}\,K^{-1}$. The crossover from the cubic to the linear dependence thus occurs at $T_{co}\approx53$ K, very much independent of

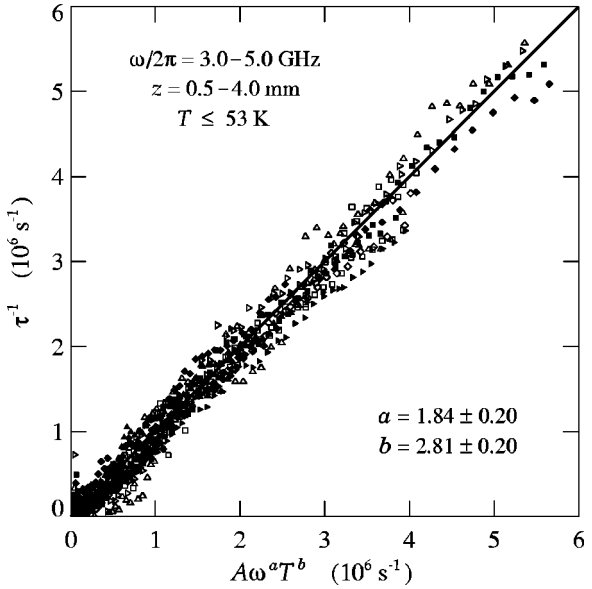

FIG. 3. Plot of all data points below $T_{co} \approx 53$ K versus $A\omega^a T^b$, after conversion of the measured Brillouin intensity to τ^{-1} by use of Eq. (3). The figure demonstrates the validity of Eq. (1). The phonon frequencies cover the range 3.0–5.0 GHz. The travel distance z is 2.0 mm in most cases, but data at $z = 0.5$, 1.0, 3.0, and 4.0 mm are included as well.

the frequency (Fig. 1). This crossover temperature seems reasonable in relation to the Debye temperature of TeO_2, which from acoustic[14] and crystallographic data[17] is estimated at roughly 200 K. Already around T_{co}, therefore, the thermally excited phonon spectrum, which in the Debye approximation scales with $\omega^2/[\exp(\hbar\omega/k_B T)-1]$, reaches its maximum near the zone boundary.

Finally, we once more resort to Fig. 2, to explain why the case of TeO_2 is indeed close to the asymptotic limit of small ω assumed in Herring's theory. In this connection it should first be pointed out that Fig. 2 distorts reality in the sense that, at the relevant temperatures, the ST and FT phonons taking part in the scattering process are two orders of magnitude further out into the Brillouin zone. However, the excessive anisotropy of the ST slowness surface remains preserved, and the energy and wave-vector separation of the ST and FT contours remains determined by the L phonon. Under these conditions, the participating ST and FT phonons are essentially confined to wave vectors only 1° away from the degeneracy. Owing to the strong anisotropy, therefore, the situation is quite different from systems like Al_2O_3 and MgO,[12] where the eccentricity of the ST and FT slowness surfaces is limited to about 5%, and, at least for frequencies in the gigahertz range, the locus of the $\mathbf{q}_1$ conserving momentum and energy occurs at angles of several tens of degrees.

V. CONCLUSIONS

In summary, we have measured the attenuation of longitudinal phonons propagating along the [001] axis in a single crystal of TeO_2 as a function of the frequency and the temperature. The primary conclusion is that the phonon relaxation confirms the theory for phonon attenuation in anisotropic crystals by Herring.[1]

ACKNOWLEDGMENTS

The work was supported by the Netherlands Foundation ''Fundamenteel Onderzoek der Materie (FOM)'' and the ''Nederlandse Organisatie voor Wetenschappelijk Onderzoek (NWO).''

[1] C. Herring, Phys. Rev. **95**, 954 (1954).
[2] J. W. Tucker and V. W. Rampton, *Microwave Ultrasonics in Solid State Physics* (North-Holland, Amsterdam, 1972).
[3] *Nonequilibrium Phonons in Nonmetallic Crystals*, edited by W. Eisenmenger and A. A. Kaplyanskii (North-Holland, Amsterdam, 1986).
[4] G. P. Srivastava, *The Physics of Phonons* (Adam Hilger, Bristol, 1990).
[5] J. Callaway, Phys. Rev. **113**, 1046 (1959).
[6] P. Carruthers, Rev. Mod. Phys. **33**, 92 (1961).
[7] M. G. Holland, Phys. Rev. **132**, 2461 (1963).
[8] R. Bergman, *Thermal Conduction of Solids* (Oxford University Press, Oxford, 1976).
[9] Y.-J. Han and P. G. Klemens, Phys. Rev. B **48**, 6033 (1993).
[10] For a recent comprehensive experimental study, critically reviewing the $\omega^a T^b$ dependences of the various phonon decays, see M. Asen-Palmer, K. Bartkowski, E. Gmelin, M. Cardona, A. P. Zhernov, A. V. Inyushkin, A. Taldenkov, V. I. Ozhogin, K. M. Itoh, and E. E. Haller, Phys. Rev. B **56**, 9431 (1997).
[11] E. P. N. Damen, A. F. M. Arts, and H. W. de Wijn, Phys. Rev. Lett. **74**, 4249 (1995). This technique of phonon generation is viable also at low temperatures, because the reduced specific heat of the metallic transducer makes up for the reduced thermal expansion and conductivity.
[12] I. S. Ciccarello and K. Dransfeld, Phys. Rev. **134**, A1517 (1964).
[13] H. J. Maris, Philos. Mag. **9**, 901 (1964).
[14] Y. Ohmachi and N. Uchida, J. Appl. Phys. **41**, 2307 (1970).
[15] G. A. Coquin, D. A. Pinnow, and A. W. Warner, J. Appl. Phys. **42**, 2162 (1971).
[16] J. M. Farley, G. A. Saunders, and D. Y. Chung, J. Phys. C **8**, 780 (1975).
[17] J. Leciejewicz, Z. Kristallogr. **116**, 345 (1961).
[18] Another noteworthy point, quite unique for TeO_2, is that the L slowness surface intersects one of the iso-energetic T surfaces along degeneracy lines of type (iii). These however yield a non-dominant contribution with $a = 3$.
[19] Similar data in $PbMoO_4$, which has crystal class C_{4h}, yielded $a = 1.95 \pm 0.10$.